Differential Sensitivity of the KM3NeT/ARCA detector to a diffuse neutrino flux and to point-like source emission: Exploring the case of the Starburst Galaxies

S. Aiello [1], A. Albert [2,52], M. Alshamsi [4,3], S. Alves Garre [5], Z. Aly [3], A. Ambrosone [7,6,*], F. Ameli [8], M. Andre [9], E. Androutsou [10], M. Anguita [11], L. Aphecetche [12], M. Ardid [13], S. Ardid [13], H. Atmani [14], J. Aublin [15], F. Badaracco [16], L. Bailly-Salins [17], Z. Bardačová [19,18], B. Baret [15], A. Bariego-Quintana [5], S. Basegmez du Pree [20], Y. Becherini [15], M. Bendahman [14,15], F. Benfenati [22,21], M. Benhassi [23,6], D.M. Benoit [24], E. Berbee [20], V. Bertin [3], S. Biagi [25], M. Boettcher [26], D. Bonanno [25], J. Boumaaza [14], M. Bouta [27], M. Bouwhuis [20], C. Bozza [28,6], R.M. Bozza [7,6], H.Brânzaş [29], F. Bretaudeau [12], M. Breuhaus [3], R. Bruijn [30,20], J. Brunner [3], R. Bruno [1], E. Buis [31,20], R. Buompane [23,6], J. Busto [3], B. Caiffi [16], D. Calvo [5], S. Campion [8,32], A. Capone [8,32], F. Carenini [22,21], V. Carretero [5], T. Cartraud [15], P. Castaldi [33,21], V. Cecchini [5], S. Celli [8,32], L. Cerisy [3], M. Chabab [34], M. Chadolias [35], A. Chen [36], S. Cherubini [37,25], T. Chiarusi [21], M. Circella [38], R. Cocimano [25], J.A.B. Coelho [15], A. Coleiro [15], R. Coniglione [25], P. Coyle [3], A. Creusot [15], G. Cuttone [25], R. Dallier [12], Y. Darras [35], A. De Benedittis [6], B. De Martino [3], V. Decoene [12], R. Del Burgo [6], I. Del Rosso [22,21], L.S. Di Mauro [25], I. Di Palma [8,32], A.F. Díaz [11], C. Diaz [11], D. Diego-Tortosa [25], C. Distefano [25], A. Domi [35], C. Donzaud [15], D. Dornic [3], M. Dörr [39], E. Drakopoulou [10], D. Drouhin [2,52], R. Dvornický [19], T. Eberl [35], E. Eckerová [19,18], A. Eddymaoui [14], T. van Eeden [20], M. Eff [15], D. van Eijk [20], I. El Bojaddaini [27], S. El Hedri [15], A. Enzenhöfer [3], G. Ferrara [25], M.D. Filipović [40], F. Filippini [22,21], D. Franciotti [25], L.A. Fusco [28,6], J. Gabriel [17], S. Gagliardini [8], T. Gal [35], J. García Méndez [13], A. Garcia Soto [5], C. Gatius Oliver [20], N. Geißelbrecht [35], H. Ghaddari [27], L. Gialanella [6,23], B.K. Gibson [24], E. Giorgio [25], I. Goos [15], P. Goswami [15], D. Goupilliere [17], S.R. Gozzini [5], R. Gracia [35], K. Graf [35], C. Guidi [41,16], B. Guillon [17], M. Gutiérrez [42], H. van Haren [43], A. Heijboer [20], A. Hekalo [39], L. Hennig [35], J.J. Hernández-Rey [5], W. Idrissi Ibnsalih [6,**], G. Illuminati [22,21], M. de Jong [44,20], P. de Jong [30,20], B.J. Jung [20], P. Kalaczyński [45,53], O. Kalekin [35], U.F. Katz [35], G. Kistauri [47,46], C. Kopper [35], A. Kouchner [48,15], V. Kueviakoe [20], V. Kulikovskiy [16], R. Kvatadze [47], M. Labalme [17], R. Lahmann [35], G. Larosa [25], C. Lastoria [3], A. Lazo [5], S. Le Stum [3], G. Lehaut [17], E. Leonora [1], N. Lessing [5], G. Levi [22,21], M. Lindsey Clark [15], F. Longhitano [1], F. Magnani [3], J. Majumdar [20], L. Malerba [16], F. Mamedov [18], J. Mańczak [5], A. Manfreda [6], M. Manzaneda [5], M. Marconi [41,16], A. Margiotta [22,21], A. Marinelli [7,6,**], C. Markou [10], L. Martin [12], J.A. Martínez-Mora [13], F. Marzaioli [23,6], M. Mastrodicasa [32,8], S. Mastroianni [6], S. Miccichè [25], G. Miele [7,6], P. Migliozzi [6], E. Migneco [25], M.L. Mitsou [6], C.M. Mollo [6], L. Morales-Gallegos [23,6], M. Morga [38], A. Moussa [27], I. Mozun Mateo [17], R. Muller [20], M.R. Musone [6,23], M. Musumeci [25], S. Navas [42], A. Nayerhoda [38],

* Corresponding author at: INFN, Sezione di Napoli, Complesso Universitario di Monte S. Angelo, Via Cintia ed. G, Napoli, 80126, Italy.
** Corresponding authors.
    E-mail addresses: antonio.ambrosone@unina.it (A. Ambrosone), walid.idrissiibnsalih@unicampania.it (W.I. Ibnsalih), antonio.marinelli@unina.it (A. Marinelli), km3net-pc@km3net.de (K. Collaboration).

C.A. Nicolau [8], B. Nkosi [36], B. Ó Fearraigh [30,20], V. Oliviero [7,6], A. Orlando [25], E. Oukacha [15], D. Paesani [25], J. Palacios González [5], G. Papalashvili [38,46], V. Parisi [41,16], E.J. Pastor Gomez [5], A.M. Păun [29], G.E. Păvălaș [29], S. Peña Martínez [15], M. Perrin-Terrin [3], J. Perronnel [17], V. Pestel [17], R. Pestes [15], P. Piattelli [25], C. Poirè [28,6], V. Popa [29], T. Pradier [2], J. Prado [5], S. Pulvirenti [25], G. Quéméner [17], C.A. Quiroz-Rangel [13], U. Rahaman [5], N. Randazzo [1], R. Randriatoamanana [12], S. Razzaque [49], I.C. Rea [6], D. Real [5], G. Riccobene [25], J. Robinson [26], A. Romanov [41,16], A. Šaina [5], F. Salesa Greus [5], D.F.E. Samtleben [44,20], A. Sánchez Losa [5,38], S. Sanfilippo [25], M. Sanguineti [41,16], C. Santonastaso [23,6], D. Santonocito [25], P. Sapienza [25], J. Schnabel [35], J. Schumann [35], H.M. Schutte [26], J. Seneca [20], N. Sennan [27], B. Setter [35], I. Sgura [38], R. Shanidze [46], A. Sharma [15], Y. Shitov [18], F. Šimkovic [19], A. Simonelli [6], A. Sinopoulou [1], M.V. Smirnov [35], B. Spisso [6], M. Spurio [22,21], D. Stavropoulos [10], I. Štekl [18], M. Taiuti [41,16], Y. Tayalati [14], H. Thiersen [26], I. Tosta e Melo [1,37], E. Tragia [10], B. Trocmé [15], V. Tsourapis [10], A. Tudorache [8,32], E. Tzamariudaki [10], A. Vacheret [17], A. Valer Melchor [20], V. Valsecchi [25], V. Van Elewyck [48,15], G. Vannoye [3], G. Vasileiadis [50], F. Vazquez de Sola [20], C. Verilhac [15], A. Veutro [8,32], S. Viola [25], D. Vivolo [23,6], J. Wilms [51], E. de Wolf [30,20], H. Yepes-Ramirez [13], G. Zarpapis [10], S. Zavatarelli [16], A. Zegarelli [8,32], D. Zito [25], J.D. Zornoza [5], J. Zúñiga [5], N. Zywucka [26], KM3NeT Collaboration

[1] *INFN, Sezione di Catania, (INFN-CT), Via Santa Sofia 64, Catania, 95123, Italy*

[2] *Université de Strasbourg, CNRS, IPHC UMR 7178, F-67000 Strasbourg, France*

[3] *Aix Marseille Univ, CNRS/IN2P3, CPPM, Marseille, France*

[4] *University of Sharjah, Sharjah Academy for Astronomy, Space Sciences, and Technology, University Campus - POB 27272, Sharjah, United Arab Emirates*

[5] *IFIC - Instituto de Fí,sica Corpuscular (CSIC - Universitat de València), c/Catedrático José Beltrán, 2, 46980 Paterna, Valencia, Spain*

[6] *INFN, Sezione di Napoli, Complesso Universitario di Monte S. Angelo, Via Cintia ed. G, Napoli, 80126, Italy*

[7] *Università di Napoli "Federico II", Dip. Scienze Fisiche "E. Pancini", Complesso Universitario di Monte S. Angelo, Via Cintia ed. G, Napoli, 80126, Italy*

[8] *INFN, Sezione di Roma, Piazzale Aldo Moro 2, Roma, 00185, Italy*

[9] *Universitat Politècnica de Catalunya, Laboratori d'Aplicacions Bioacústiques, Centre Tecnològic de Vilanova i la Geltrú, Avda. Rambla Exposició, s/n, Vilanova i la Geltrú, 08800, Spain*

[10] *NCSR Demokritos, Institute of Nuclear and Particle Physics, Ag. Paraskevi Attikis, Athens, 15310, Greece*

[11] *University of Granada, Dept. of Computer Architecture and Technology/CITIC, 18071 Granada, Spain*

[12] *Subatech, IMT Atlantique, IN2P3-CNRS, Nantes Université, 4 rue Alfred Kastler - La Chantrerie, Nantes, BP 20722 44307, France*

[13] *Universitat Politècnica de València, Instituto de Investigación para la Gestión Integrada de las Zonas Costeras, C/ Paranimf, 1, Gandia, 46730, Spain*

[14] *University Mohammed V in Rabat, Faculty of Sciences, 4 av. Ibn Battouta, B.P. 1014, R.P. 10000 Rabat, Morocco*

[15] *Université Paris Cité, CNRS, Astroparticule et Cosmologie, F-75013 Paris, France*

[16] *INFN, Sezione di Genova, Via Dodecaneso 33, Genova, 16146, Italy*

[17] *LPC CAEN, Normandie Univ, ENSICAEN, UNICAEN, CNRS/IN2P3, 6 boulevard Maréchal Juin, Caen, 14050, France*

[18] *Czech Technical University in Prague, Institute of Experimental and Applied Physics, Husova 240/5, Prague, 110 00, Czech Republic*

[19] *Comenius University in Bratislava, Department of Nuclear Physics and Biophysics, Mlynska dolina F1, Bratislava, 842 48, Slovak Republic*

[20] *Nikhef, National Institute for Subatomic Physics, PO Box 41882, Amsterdam 1009 DB, Netherlands*

[21] *INFN, Sezione di Bologna, v.le C. Berti-Pichat, 6/2, Bologna, 40127, Italy*

[22] *Università di Bologna, Dipartimento di Fisica e Astronomia, v.le C. Berti-Pichat, 6/2, Bologna, 40127, Italy*

[23] *Università degli Studi della Campania "Luigi Vanvitelli", Dipartimento di Matematica e Fisica, viale Lincoln 5, Caserta, 81100, Italy*

[24] *E.A. Milne Centre for Astrophysics, University of Hull, Hull, HU6 7RX, United Kingdom*

[25] *INFN, Laboratori Nazionali del Sud, (LNS) Via S. Sofia 62, Catania, 95123, Italy*

[26] *North-West University, Centre for Space Research, Private Bag X6001, Potchefstroom, 2520, South Africa*

[27] *University Mohammed I, Faculty of Sciences, BV Mohammed VI, B.P. 717, R.P. 60000 Oujda, Morocco*

[28] *Università di Salerno e INFN Gruppo Collegato di Salerno, Dipartimento di Fisica, Via Giovanni Paolo II 132, Fisciano, 84084, Italy*

[29] *ISS, Atomistilor 409, Măgurele, RO 077125, Romania*

[30] *University of Amsterdam, Institute of Physics/IHEF, PO Box 94216, Amsterdam 1090 GE, Netherlands*

[31] *TNO, Technical Sciences, PO Box 155, Delft 2600 AD, Netherlands*

[32] *Università La Sapienza, Dipartimento di Fisica, Piazzale Aldo Moro 2, Roma, 00185, Italy*

[33] *Università di Bologna, Dipartimento di Ingegneria dell'Energia Elettrica e dell'Informazione "Guglielmo Marconi", Via dell'Università 50, Cesena, 47521, Italy*

[34] *Cadi Ayyad University, Physics Department, Faculty of Science Semlalia, Av. My Abdellah, P.O.B. 2390, Marrakech, 40000, Morocco*

[35] *Friedrich-Alexander-Universität Erlangen-Nürnberg (FAU), Erlangen Centre for Astroparticle Physics, Nikolaus-Fiebiger-Straße 2, 91058 Erlangen, Germany*

[36] *University of the Witwatersrand, School of Physics, Private Bag 3, Johannesburg, Wits 2050, South Africa*

[37] *Università di Catania, Dipartimento di Fisica e Astronomia "Ettore Majorana", (INFN-CT), Via Santa Sofia 64, Catania, 95123, Italy*

[38] *INFN, Sezione di Bari, via Orabona, 4, Bari, 70125, Italy*

[39] *University Würzburg, Emil-Fischer-Straße 31, Würzburg, 97074, Germany*

[40] *Western Sydney University, School of Computing, Engineering and Mathematics, Locked Bag 1797, Penrith, NSW 2751, Australia*

[41] *Università di Genova, Via Dodecaneso 33, Genova, 16146, Italy*

[42] *University of Granada, Dpto. de Fí,sica Teórica y del Cosmos & C.A.F.P.E., 18071 Granada, Spain*

[43] *NIOZ (Royal Netherlands Institute for Sea Research), PO Box 59, Den Burg, Texel 1790 AB, The Netherlands*

[44] *Leiden University, Leiden Institute of Physics, PO Box 9504, Leiden 2300 RA, Netherlands*

[45] *National Centre for Nuclear Research, 02-093 Warsaw, Poland*

[46] *Tbilisi State University, Department of Physics, 3, Chavchavadze Ave., Tbilisi, 0179, Georgia*

[47] *The University of Georgia, Institute of Physics, Kostava str. 77, Tbilisi, 0171, Georgia*

[48] *Institut Universitaire de France, 1 rue Descartes, Paris, 75005, France*

[49] *University of Johannesburg, Department Physics, PO Box 524, Auckland Park 2006, South Africa*

[50] *Laboratoire Univers et Particules de Montpellier, Place Eugène Bataillon-CC 72, Montpellier Cédex 05 34095, France*

[51] *Friedrich-Alexander-Universität Erlangen-Nürnberg (FAU), Remeis Sternwarte, Sternwartstraße 7, 96049 Bamberg, Germany*

[52] *Université de Haute Alsace, rue des Frères Lumière, 68093 Mulhouse Cedex, France*

53 *AstroCeNT, Nicolaus Copernicus Astronomical Center, Polish Academy of Sciences, Rektorska 4, Warsaw, 00-614, Poland*

ARTICLE INFO

ABSTRACT

KM3NeT/ARCA is a Cherenkov neutrino telescope under construction in the Mediterranean sea, optimised for the detection of astrophysical neutrinos with energies above ∼1 TeV. In this work, using Monte Carlo simulations including all-flavour neutrinos, the integrated and differential sensitivities for KM3NeT/ARCA are presented considering the case of a diffuse neutrino flux as well as extended and point-like neutrino sources. This analysis is applied to Starburst Galaxies demonstrating that the detector has the capability of tracing TeV neutrinos from these sources. Remarkably, after eight years, a hard power-law spectrum from the nearby Small Magellanic Cloud can be constrained. The sensitivity and discovery potential for NGC 1068 is also evaluated showing that KM3NeT/ARCA will discriminate between different astrophysical components of the measured neutrino flux after 3 years of data taking.

1. Introduction

The KM3NeT research infrastructure [1] is comprised of two deep-sea Cherenkov neutrino telescopes under construction in the Mediterranean Sea: ARCA (Astroparticle Research with Cosmics in the Abyss) located 3500 m below the sea level, off shore the coast of Capo Passero (Sicily, Italy) and ORCA (Oscillation Research with Cosmics in the Abyss) installed at a sea-bottom depth of ∼2500 m off shore Toulon (France). ARCA will have an instrumented volume of about 1 km^3 and its geometry is optimised to detect high-energy astrophysical neutrinos above ∼1 TeV, while ORCA is designed to study GeV neutrino physics analysing oscillation patterns of atmospheric neutrinos. The detection principle for neutrinos[1] in KM3NeT is based on the observation of the Cherenkov light induced in the sea water by secondary charged particles produced in the interaction of neutrinos inside or in the surroundings of the detector. Given the excellent optical seawater properties, the experiment will reach unprecedented angular resolution in the identification of neutrino sources.

In this paper, the detection performance of the full ARCA telescope, both for a diffuse neutrino flux and individual sources, are explored. Using Monte Carlo simulations for all neutrino flavours, the energy-dependent 90% confidence level (CL) sensitivity for ARCA is calculated, exploiting both track-like and shower-like events. Track-like (referred to as *tracks*) events are mainly due to charged current (CC) muon neutrino interactions; shower-like (referred to as *showers*) events are mostly due to neutral current and electron neutrinos charged current interactions.

For the track-like events, only upgoing events are considered, using the Earth as a shield to reduce the atmospheric muon contamination. Shower-like events are selected from the whole sky, using a containment requirement in the fiducial volume of the detector in order to limit the contamination from atmospheric muons and neutrinos. This selected sample is used to test if ARCA is able to identify TeV neutrinos from Starburst Galaxies (SBGs), either as a contribution to the diffuse flux or as emission from individual sources. SBGs are galaxies experiencing intense phases of star formation activity, which leads to an increased rate of supernova explosions. This enhanced activity is expected to accelerate cosmic rays up to ∼PeV energies and copiously produce gamma-rays and neutrinos [2–4]. In the diffuse flux analysis, the SBG diffuse emission up to a redshift of ∼4 is considered [2]. In the individual source analysis, the Small Magellanic Cloud (SMC), the Circinus Galaxy [3] and NGC1068 [5] have been analysed.

The paper is organised as follows: in Section 2, the event simulation and selection are outlined. In Section 3, the statistical analysis framework is presented. In particular, in Section 3.1, the definition of the sensitivity is discussed, while in Section 3.2, the differential limits are introduced and compared with the integrated limits.

---

[1] In this paper, the word neutrino is used to refer to both neutrinos and antineutrinos.

2. Event simulation and selection

Neutrino event interactions in the proximity of the ARCA detector are generated through the gSeaGen package [6]. The atmospheric muon flux is simulated using the MUPAGE code [7]. Monte Carlo simulations continue propagating charged particles emerging from neutrino interactions and atmospheric muon tracks through the active volume of the detector and reproducing the response of the front end electronics. The simulated data stream is filtered and reconstructed with the same algorithms used for real data. For this analysis, both upgoing tracks and all-sky showers samples are used, following the event selection discussed in [8]. For the final selection, two dedicated boosted decision trees are trained in order to reject mis-reconstructed events in each sample. The neutrino purity of the two final samples is 99% for tracks and 61% for showers. Moreover, the selection preserves 95% of the signal neutrinos for tracks and 70% of the signal neutrinos for showers [8]. The final background distribution accounts for atmospheric neutrinos and muons.

3. Analysis framework

3.1. Sensitivity definition

In this paper, a binned maximum likelihood ratio method is used to evaluate the ARCA sensitivity. Following the formalism and the notation of [9], the likelihood function is defined as

$$\mathscr{L} = \prod_i P(n_i, \mu_i) \tag{1}$$

with $\mu_i = \lambda \cdot \mu_s^i + \mu_b^i$

where $P(n, \mu)$ is the Poisson probability distribution (PDF) of observing n events with mean value μ, μ_s is the expected number of signal events, while μ_b is the expected number of background events. The index i runs over bins of reconstructed variables. For the following, the events are binned in reconstructed energy for the diffuse flux analysis and reconstructed energy and angular distance of the events to the source for the point-like analysis (see below for further details). The signal strength λ is left as a free normalisation parameter. Data samples are simulated by means of pseudo-experiments (PEs) generation. The procedure consists of randomly generating events according to PDFs of the signal and the background and then evaluating the test statistic (TS) for each PE. The TS is defined as

$$TS = \frac{\mathscr{L}(\tilde{\lambda})}{\mathscr{L}(\lambda = 0)} \tag{2}$$

where $\tilde{\lambda}$ is the signal strength value which maximises the likelihood for a given PE. The 90% CL sensitivity is defined as the signal strength (λ_{90}) for which 90% of the signal is above the median of the background-only distribution. Namely,

$$\int_{TS_m}^{+\infty} d(TS|\lambda_{90}) \, dTS = 90\% \tag{3}$$

where TS_m is the median distribution in the null hypothesis (only background) and $d(TS|\lambda_{90})$ is the PDF distribution of the TS for a given λ_{90} value. Generally, λ_{90} is referred to as Model Rejection Factor (MRF), because, when signal simulations are performed according to a theoretical model, a MRF ≤ 1 indicates an effective 90% CL constraint on that model. On the other hand, the model discovery potential (MDP), also called the discovery flux, is defined as the minimum flux needed for a discovery with 5σ significance level in 50% of the cases.

$$\int_{TS_{5\sigma}}^{+\infty} d(TS|\lambda_{5\sigma}) \, dTS = 50\% \tag{4}$$

where $TS_{5\sigma} = 2.85 \cdot 10^{-7}$ is the TS threshold corresponding to a 5σ significance. This value is calculated using the one-sided Gaussian approximation [10]. The final sensitivity is defined as

$$\phi_{90}(E) = \lambda_{90}\phi_s(E) \tag{5}$$

while the discovery flux as

$$\phi_{5\sigma}(E) = \lambda_{5\sigma}\phi_s(E) \tag{6}$$

where $\phi_s(E)$ is the signal flux injected in the simulations corresponding to $\lambda = 1$. Typically, the injected signal spectrum $\phi_s(E)$ is modelled as a power-law $E^{-\gamma}$, resulting in sensitivity and MDP profiles mirroring the shape of the injected spectrum. In fact, Eqs. (5) and (6) provide results depending solely on the spectral shape and are entirely independent of the specific scaling or normalisation of the injected signal. Such expectations are also referred to as energy-integrated expectations, see [8].

3.2. Differential sensitivity and discovery flux

The differential sensitivity and discovery flux (in general, referred to as 'differential limits') correspond to the performance of a detector for a given energy range [9]. In other words, they represent the minimum differential signal neutrino flux that the detector can either constrain or discover. They are only mildly model-dependent and represent important instrument response functions. In order to evaluate them, the signal is divided in bins of logarithm of true energy, injecting an E^{-2} spectrum within each bin. The width of the bins is chosen to be half decade in energy.[2] Since the sensitivity is inversely proportional to the number of signal events n_s provided by the injected spectrum [11], there is a strict connection between differential and integrated sensitivities. In particular,

$$\lambda_{90} \propto n_s^{-1} = \frac{1}{\sum_i n_s^i} \propto \frac{1}{\sum_i (\lambda_{90}^i)^{-1}} \tag{7}$$

where λ_{90} is the integrated MRF, i runs over the number of energy bins and λ_{90}^i is the MRF for each energy bin of the signal.

The integrated MRF, as shown in Eq. (7), is always smaller than the differential MRF. In fact, in differential limits, each individual energy bin is treated as independent, assuming a zero signal flux outside the bin. This results in the same amount of background events within each bin, leading to worse limits. The integrated sensitivity exploits the energy dependence of the flux to distinguish between the signal and the background, while the differential sensitivity provides the generic differential flux which the detector can discriminate, leading to a more stringent requirement. On the other hand, the differential limits better highlight the energy range where the detector is most sensitive, especially for different event samples (tracks and showers).

In the following, these quantities are computed and discussed in the context of the sensitivity of ARCA to neutrino emission from starburst galaxies.

---

[2] Injecting softer spectra such as $E^{-2.1} - E^{-2.2}$ changes the overall sensitivity of $\sim 2-3\%$ leaving the results unchanged.

4. Diffuse analysis

The 90% CL differential sensitivity for a diffuse neutrino flux both for the upgoing tracks (orange dashed line) and all-sky showers (red dashed–dotted line) is shown in Fig. 1. For comparison, the 1σ bands around the diffuse neutrino flux from SBGs predicted by [2] from SBGs are also reported. Predictions shown in the left (right) panel are obtained through a multi-component fit of the extragalactic gamma-ray background measured by Fermi-LAT [12] and the 7.5 yr HESE neutrino flux [13] (6 yr shower neutrino flux [14]) measured by IceCube (see [2] for further details).

The sensitivities refer to 10 years of data collected by the ARCA detector for one single flavour of neutrinos. For neutrino energies below 100 TeV, the sensitivity is predominantly driven by purely upgoing events ($\theta \leq 80°$), where θ is the reconstructed zenith angle of the tracks and $\theta = 0°$ corresponds to a vertical upgoing track. For energies exceeding 100 TeV, the sensitivity is dominated by horizontal events ($80° < \theta < 100°$) due to neutrino absorption in the Earth. This results in a minimum of the sensitivity around 1 PeV. The minimum of the sensitivity for showers is at $\simeq 100$ TeV because the event containment significantly reduces the amount of observed signal above this energy. Due to a reduced background rate, the shower sensitivity is better than the one for tracks for $E_\nu \lesssim 100$ TeV. For $E_\nu \gtrsim 100$ TeV, the sensitivity is dominated by the tracks, because of a larger effective volume for track-like events as the energy increases. After 10 years of operation, ARCA will probe the neutrino emission from SBGs, either confirming or constraining their contribution to the diffuse neutrino flux around ~ 100 TeV. The sensitivities shown in Fig. 1 suggest that ARCA will also improve the characterisation of the diffuse neutrino flux provided by IceCube [13,14], thus providing valuable information regarding other astrophysical sources contributing to the diffuse neutrino flux such as gamma-ray opaque sources [15].

5. Point-like SBG analysis

ARCA is expected to have an excellent angular resolution ($\lesssim 0.2°$ for tracks and $E_\nu \geq 10$ TeV see [8], and therefore an enhanced sensitivity for point-like and extended sources. The likelihood function takes into account both the reconstructed energy (E_{rec}) and the angular distance between the nominal position of the source and the reconstructed direction of the event within an angle α. The range $[10, 10^8]$ GeV and $[0, 5°]$ ($[0, 15°]$) for tracks (showers) are respectively considered for the reconstructed energy and α. In the following, the evaluation of the differential limits is performed considering the position of three local SBGs in order to test the ability of ARCA to trace their star-forming activity through neutrino emission. Specifically, the Small Magellanic Cloud and the Circinus Galaxy are studied, because their expected neutrino fluxes should be high enough to match ARCA sensitivity after ~ 6 years of operation [3]. The case of NGC 1068, whose neutrino emission has been measured by IceCube at 4.2σ significance with a neutrino flux normalisation $\phi_{\nu_\mu + \bar{\nu}_\mu} = 5.0 \times 10^{-11}$ TeV^{-1} cm^{-2} s^{-1} at $E_\nu = 1$ TeV [5], is also considered.

5.1. Small magellanic cloud

The Small Magellanic Cloud is a local star-forming galaxy at a distance of ~ 60 kpc [16], characterised by a stable and diffuse gamma-ray emission, driven by its star-forming activity [17]. Its expected neutrino emission has been estimated using a one-zone model tuned to its gamma-ray spectrum by [3]. The capability of ARCA to test this model is evaluated by simulating the SMC as an extended source with a radius $r = 0.5°$, consistent with its angular extension measured by the Fermi-LAT Collaboration [17].

The 90% CL differential sensitivity and the 5σ differential discovery flux for the SMC, considering 10 years of ARCA operation, are shown
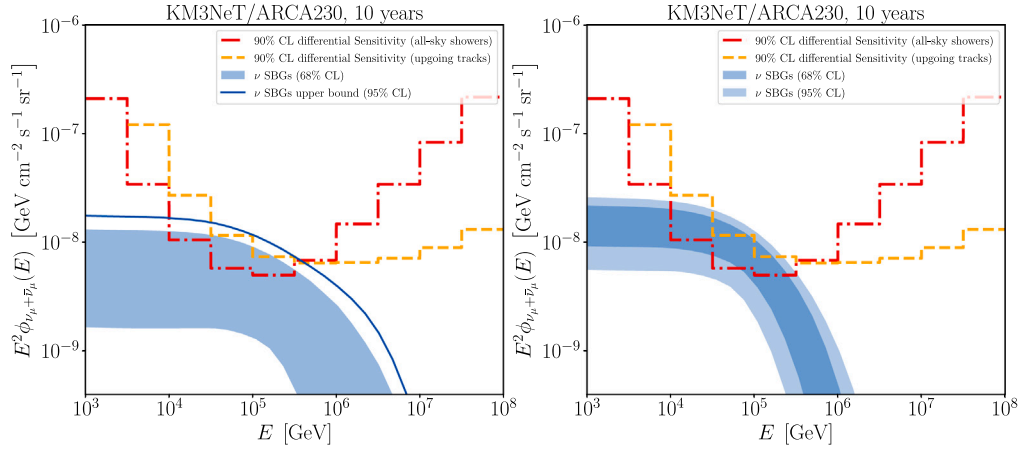
Fig. 1. 90% CL differential sensitivity to a diffuse neutrino flux for the sample of upgoing tracks (dashed orange) and of all-sky showers (dashed–dotted red). On the left, the sensitivities are compared to the theoretical 1σ band prediction for SBGs neutrino as obtained in [2] through a multi-component fit of the extragalactic gamma-ray background (EGB) measured by Fermi-LAT [12], and the 7.5 yr HESE neutrino flux measured by IceCube [13]. On the right, the KM3NeT/ARCA expectations are compared to the blue band which corresponds to the 1σ SBG neutrino expectations from [2] obtained by a multi-component fit of the EGB measured by Fermi-LAT [12] and the 6-yr shower neutrino flux measured by IceCube [14].
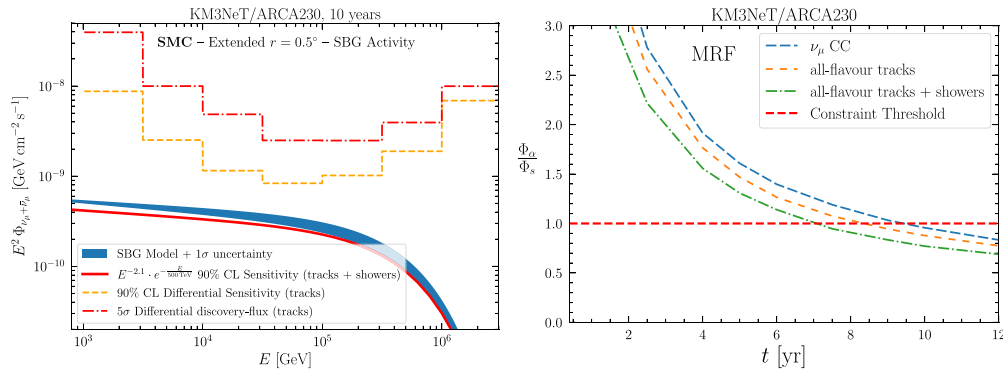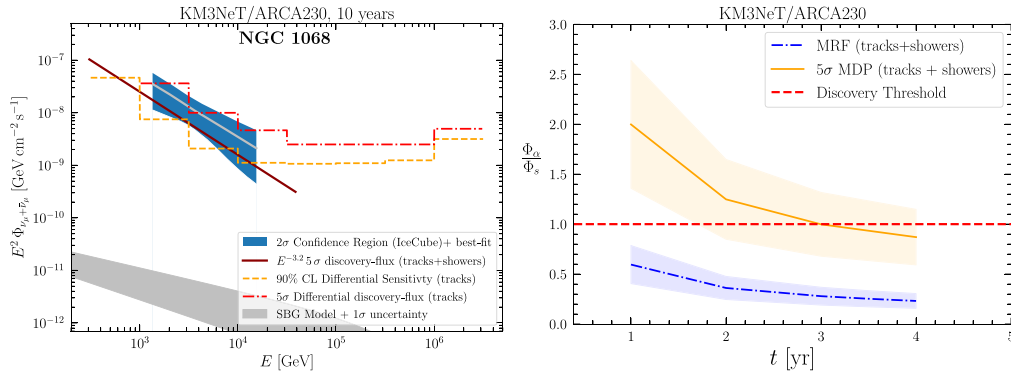

Fig. 2. Left: 90% differential sensitivity (orange dashed line) and the 5σ differential discovery flux (red dashed–dotted line) of ARCA after 10 years of operation for one neutrino flavour compared with the 1σ SBG neutrino model (blue band) from [3]. The energy-integrated sensitivity (tracks+showers) for the best-fit spectrum of the source (considering 10 years of operation) is also reported. Right: energy-integrated MRF (best fit flux) as a function of time for different event samples. The blue line refers to ν_μ CC events, orange to the all-flavour tracks, and green to tracks+showers.

in the left panel of Fig. 2 and compared with the 1σ neutrino expectations from [3]. The track+shower energy-integrated sensitivity is also reported for the best-fit spectrum of the source which can be described by a power-law with an exponential cutoff $\sim E^{-2.1} \cdot e^{(-E/500\ \text{TeV})}$. The cutoff at 500 TeV comes from the assumption of maximal proton energy $\simeq 10$ PeV. In the right panel of Fig. 2, The energy-integrated MRF is shown as a function of time. Three different event samples are considered: ν_μ in CC, all-flavour tracks (ν_μ CC interactions and ν_τ in CC interactions where the τ decays into a muon) and finally all-flavour tracks + showers. The horizontal threshold line (MRF = 1) is superimposed for comparison. Although the detector is not sensitive to discriminate the flux in single true energy signal bins, the integrated spectrum can be constrained after ~ 8 years, combining the information from the track-like and shower-like sample. The samples provide different results due to a diverse amount of events (signal and background) contained in each sample. Therefore, this will test the model proposed by [3]. It is important to stress that this source, having a low star formation rate, might have a sizeable contamination from leptonic point-like sources, such as pulsar wind nebulae, in its gamma-ray spectrum, leading to a smaller neutrino spectrum than the one provided in [3]. This will allow for a crucial test of the neutrino content of the source. If the neutrino emission is limited in a smaller region than the entire galaxy, the sensitivity improves, as discussed in Appendix A.

5.2. NGC 1068

NGC 1068 is a source situated at ~ 10–14 Mpc from the Milky Way [17]. It is classified as a Starburst and as a type II Seyfert galaxy, characterised by a star formation rate of ~ 23 $M_\odot$ yr^{-1} and by the presence of a starburst ring [18]. Its Seyfert activity is located mainly inside its active nucleus [17,19], and its hot corona [17,18,20–23]. The ALMA telescope [18,24,25] has also detected a powerful radio jet and four parsec-scale blobs in the jet head, which may represent sites for cosmic ray acceleration. Furthermore, a hint of an ultra-fast outflow in the core of the source has been reported by [26] analysing absorption lines in the X-ray band. Recently, the IceCube Collaboration has reported an excess of 79^{+22}_{-20} astrophysical neutrinos from the direction of NGC 1068, with an overall significance of 4.2σ above the background-only hypothesis [5]. The measured neutrino flux normalisation is at least a factor 10 above the measured gamma-ray flux [17,27], rather than the typical factor of about 2 expected from hadronic emission in transparent sources.

Both AGN and SBG activities have been used to explain the origin of such a high neutrino flux. However, the SBG-related emission produces a neutrino flux approximately two orders of magnitude below the Ice-Cube measurements [3,28]. On the other hand, AGN-related emissions can produce a greater contribution to observed neutrino flux [29–31]. At the moment, the favoured scenario seems a considerable neutrino emission related to the magnetised hot corona activity [21].

Fig. 3. Left: 90% CL differential sensitivity (orange dashed line) and 5σ differential discovery flux (red dashed–dotted line) and the energy-integrated 5σ discovery for an $E^{-3.2}$ spectrum using the tracks+showers sample (dark red line). The expectations are compared with the IceCube-measured 2σ region for the spectrum [5] (blue band) and the theoretical neutrino predictions from SBG activity according to [3] (grey band). Right: Energy-integrated 5σ discovery flux and 90% CL sensitivity as functions of the operation time based on the combined track+shower sample. The bands correspond to the uncertainty of the flux measured by [5]. After ~ 3 years, KM3NeT/ARCA is expected to confirm the spectrum measured by IceCube.
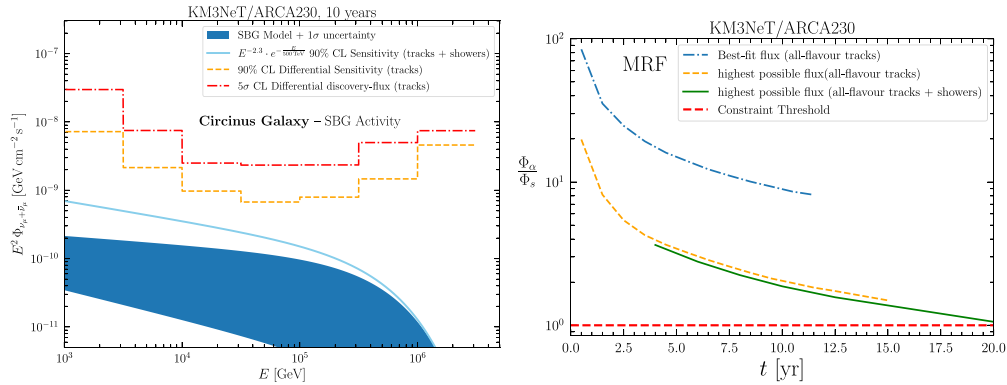
Fig. 4. Left: 90% CL track differential sensitivity (dashed orange line), 5σ track differential discovery flux (dashed–dotted red line) for 10 years of data taking with the ARCA detector, compared with the 1σ SBG neutrino flux predictions from [3] (blue band). Also shown is the energy-integrated 90% CL sensitivity for $E^{-2.3} \cdot e^{-E/500\,\text{TeV}}$, corresponding to the best-fit neutrino spectrum from SBG activity. Right: The MRF as a function of observation time for the best-fit spectrum of the source (dashed–dotted blue line, all-flavour tracks), for the highest possible flux (1σ) (dashed orange line, all-flavour tracks) and for the highest possible flux considering tracks and showers (green line).

The time-integrated expectations for ARCA are shown in Fig. 3.

In the left panel of Fig. 3, the 90% CL differential sensitivity and the 5σ discovery flux for 10 years of data-taking for ARCA are compared with the IceCube 2σ region [5] (blue band). The obtained differential limits show that ARCA can probe a neutrino flux of $E^2\phi_{\nu_\mu+\bar\nu_\mu} \sim 5 \cdot 10^{-8}$ GeV cm^{-2} s^{-1} and of $E^2\phi_{\nu_\mu+\bar\nu_\mu} \sim 10^{-9}$ GeV cm^{-2} s^{-1} at 1 TeV and 100 TeV, respectively. The energy-integrated 5σ discovery for a $E^{-3.2}$ spectrum and the expected SBG neutrino spectral energy distribution evaluated according to [3] are also shown for comparison.

In the right panel of Fig. 3, the energy-integrated discovery flux and MRF are reported as functions of observation time and compared with the discovery threshold corresponding to MDP = 1. The bands refers to the uncertainty of the flux measured by [5].

The ARCA detector is expected to confirm the flux reported as a best fit by IceCube after only ~ 3 years of data taking and to better disentangling the emission from AGN-related components from the SBG-related one.

5.3. Circinus galaxy

Circinus is a SBG located ~ 4 Mpc from the Milky Way [16] at a declination $\delta = -65.2°$ [32], where the ARCA detector is expected to have full visibility [10]. Circinus is classified as a Seyfert II galaxy [33], showing both AGN activity and a hot corona [21,34,35]. The neutrino flux emission predicted by the hot corona model can reach a flux level of $E^2\phi_{\nu_\mu+\bar\nu_\mu} \simeq 10^{-8}$ GeV cm^{-2} s^{-1} [21] above E$_\nu \sim 1$ TeV.

In the left panel of Fig. 4, the 90% CL differential sensitivity and the 5σ differential discovery flux are compared with the 1σ neutrino expectations from SBG activity [3]. The differential limits indicate that a flux of the order of $E^2\phi_{\nu_\mu+\bar\nu_\mu} \simeq 10^{-9}$ GeV cm^{-2} s^{-1} can be probed in the energy range 30−100 TeV. Therefore, a neutrino flux connected to the AGN activity can be searched for with ARCA, which may lead to the discovery of a hot corona emission like in NGC 1068. The energy-integrated sensitivity for the best-fit SBG flux ($\text{E}^{-2.3} \cdot \text{e}^{(-\text{E}/500\,\text{TeV})}$) is also reported. In the right panel of Fig. 4, the MRF is presented as a function of observation time for different cases: the best-fit flux of the source analysed with all-flavours tracks and the highest possible flux (1σ) analysed with all-flavour tracks and all-flavour tracks + showers. The obtained sensitivity shows that the latter can be constrained after ~ 20 years of observations.

6. Impact of systematic uncertainties

In this section, a brief discussion on the systematic uncertainties associated with the ARCA sensitivity is presented. Monte Carlo simulations used in this work consider the detector geometry, calibration, water optical and background characteristics discussed in [8]. Any deviation from these values might affect either the detector response, such as the energy and angular resolution, or the background event rate, leading to a change into the sensitivity. Ref. [1] shows that the most significant factors impacting the sensitivity are a 25% uncertainty on the conventional atmospheric neutrino flux and a 10% uncertainty on the effective area (which changes the energy resolution of $\sim 5-10\%$).

The resulting uncertainty on the sensitivity from these effects can be conservatively estimated by using the fact that, in background-dominated data, MRF $\propto \sqrt{n_{back}}/n_s$, where n_{back} is the expected number of background events and n_s is the expected number of signal events provided by the input spectrum [11]. Since both the numbers of events (signal and background) are proportional to the effective area, a variation of 10% leads to a 4.6% uncertainty on the sensitivity. Furthermore, conservatively assuming that the background sample is dominated by atmospheric neutrinos, an uncertainty of 25% on the background rate leads to a 12.5% uncertainty on the sensitivity. Regarding the uncertainty of the discovery flux, Ref. [10] has shown that the 25% uncertainty on the atmospheric neutrino flux leads to a +15% and −5% uncertainty. Therefore, it is expected that for the SMC, the time required to achieve a 90% CL constraint varies within $8.0^{+2.2}_{-1.7}$, years, whereas for the highest possible flux from the Circinus galaxy, it is 20 ± 5, years. In contrast, the discovery of the $E^{-3.2}$ spectrum observed by IceCube in the direction of NGC 1068 yields an estimated time of $3.0^{+1.0}_{-0.3}$, yr.

7. Final remarks and conclusions

In this paper, the expected differential sensitivity for the ARCA detector is presented for the first time for a diffuse neutrino flux and individual neutrino sources. A binned maximum likelihood formalism is applied to evaluate the 90% CL differential sensitivity and the 5σ differential discovery flux, by binning the signal flux in true energy bins of half-decade widths. The differential limits are shown to be mostly signal model-independent and complementary to the energy-integrated limits and provide crucial information regarding the energy ranges where the detector is more sensitive to neutrino signals. They are evaluated using both upgoing track-like and all-sky contained shower-like events.

The results show that ARCA will probe the shape of the diffuse flux for $E \lesssim 100$ TeV, constraining the role of sources such as SBGs and complementing the IceCube's observations of the neutrino sky.

The likelihood formalism is also applied to local SBG sources, following the flux predictions provided in [3]. After 8 years of data taking, the Small Magellanic Cloud can be observed as a 90% CL excess in the energy-integrated analysis, proving that SBGs are guaranteed neutrino emitters. ARCA expectations for NGC 1068 have been evaluated indicating that ARCA will need only ∼3 years for discovering this source with 5σ significance. This will better disentangle the AGN-related contributions from the SBG-related one, strengthening IceCube observations. Finally, the differential limits for the Circinus Galaxy are evaluated, showing that the detector can probe its potential AGN-related emission activity additional to the expected SBG neutrino flux.

CRediT authorship contribution statement

A. Ambrosone: Formal analysis. **W. Idrissi Ibnsalih:** Formal analysis. **A. Marinelli:** Supervision.

Declaration of competing interest

The authors declare that they have no known competing financial interests or personal relationships that could have appeared to influence the work reported in this paper.

Data availability

The data that has been used is confidential.

Appendix A. Impact of extension to the differential sensitivity

The differential sensitivity at the declination of the Small Magellanic Cloud after 10 years of operation of the ARCA detector (for the tracks) is shown in Fig. A.5 considering a point-like source and an extended source with $r = 0.5°$. The differential sensitivity of the extended source worsens by ∼30% with respect to the point-like source case. Therefore, in case the neutrino emission for SBGs is concentrated within their nuclei, the sensitivity is expected to be close to the one expected for point-like sources and the time required for a 90% CL excess might reduce with the one presented in the main text.
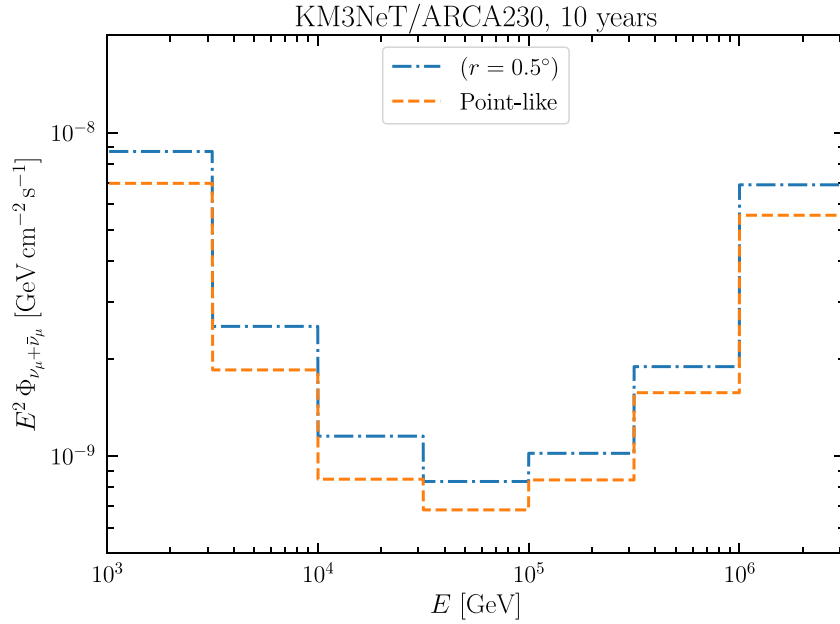
Fig. A.5. Comparison between the 90% CL differential sensitivity for a point-like source (orange dashed line) and for an extended source with an extension of $r = 0.5°$ (blue dashed–dotted line), considering 10 years of data-taking at the declination of the SMC.
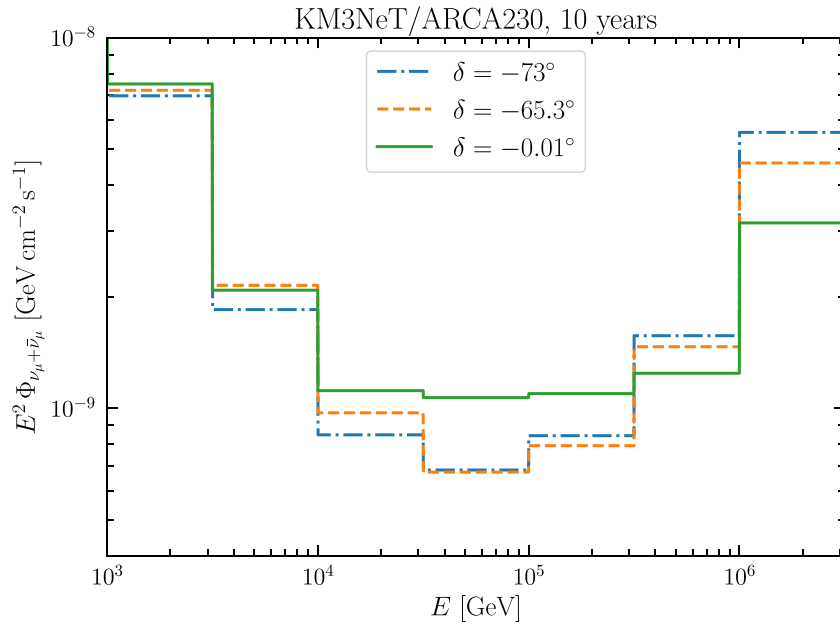

Fig. B.6. Comparison between point-like 90% CL differential sensitivity for several declinations after 10 years of operation of the ARCA detector. The blue dashed–dotted line refers to $\delta = -73°$, the orange dashed line to $\delta = -65°$ and the green line to $\delta = -0.01°$.

Appendix B. Sensitivity dependence on declination

The comparison between the differential sensitivities after 10 years of operation of ARCA is shown in Fig. B.6 for three declinations: $\delta = -73°$, $\delta = -65.3°$ and finally $\delta = -0.01°$. These declinations correspond to the positions of the SMC, Circinus Galaxy, and NGC 1068, respectively. The sensitivities for $\delta = -73°$ and $\delta = -65°$ are very close as the declination bands are also near. At high energy the sensitivity deteriorates faster for $\delta = -73°$ due to absorption from the Earth. The sensitivity at $\delta = -0.01°$ is better at high energies due to a higher signal rate, but it is worse than the others between $10-300$ TeV due to a higher background rate. In fact, $\delta = -0.01°$, the sources are only partially below the horizon (see for instance [10] for the ARCA detector visibility as a function of declination).

References

[1] S. Adrian-Martinez, et al., KM3NeT Collab, Letter of intent for KM3NeT 2.0, J. Phys. G 43 (2016) http://dx.doi.org/10.1088/0954-3899/43/8/084001, arXiv:1601.07459.

[2] A. Ambrosone, M. Chianese, D.F.G. Fiorillo, A. Marinelli, G. Miele, O. Pisanti, Starburst galaxies strike back: a multi-messenger analysis with Fermi-LAT and IceCube data, Mon. Not. R. Astron. Soc. 503 (2021) http://dx.doi.org/10.1093/mnras/stab659, arXiv:2011.02483.

[3] A. Ambrosone, M. Chianese, D.F.G. Fiorillo, A. Marinelli, G. Miele, Could nearby star-forming galaxies light up the pointlike neutrino sky? Astrophys. J. Lett. 919 (2021) http://dx.doi.org/10.3847/2041-8213/ac25ff, arXiv:2106.13248.

[4] E. Peretti, P. Blasi, F. Aharonian, G. Morlino, P. Cristofari, Contribution of starburst nuclei to the diffuse gamma-ray and neutrino flux, Mon. Not. R. Astron. Soc. 493 (2020) http://dx.doi.org/10.1093/mnras/staa698, arXiv:1911.06163.

[5] R. Abbasi, et al., Evidence for neutrino emission from the nearby active galaxy NGC 1068, Science 378 (2022) http://dx.doi.org/10.1126/science.abg3395, arXiv:2211.09972.

[6] S. Aiello, et al., KM3NeT Collab, GSeaGen: The KM3NeT GENIE-based code for neutrino telescopes, Comput. Phys. Comm. 256 (2020) http://dx.doi.org/10.1016/j.cpc.2020.107477, arXiv:2003.14040.

[7] G. Carminati, A. Margiotta, M. Spurio, Atmospheric MUons from PArametric formulas: A Fast GEnerator for neutrino telescopes (MUPAGE), Comput. Phys. Comm. 179 (2008) http://dx.doi.org/10.1016/j.cpc.2008.07.014, arXiv:0802.0562.

[8] S. Aiello, et al., KM3NeT Collab, Astronomy potential of KM3NeT/ARCA, Eur. Phys. J. C (2024) submitted for publication, arXiv:2402.08363.

[9] M.G. Aartsen, et al., Differential limit on the extremely-high-energy cosmic neutrino flux in the presence of astrophysical background from nine years of IceCube data, Phys. Rev. D 98 (2018) http://dx.doi.org/10.1103/PhysRevD.98.062003, arXiv:1807.01820.

[10] S. Aiello, et al., KM3NeT Collab, Sensitivity of the KM3NeT/ARCA neutrino telescope to point-like neutrino sources, Astropart. Phys. 111 (2019) http://dx.doi.org/10.1016/j.astropartphys.2019.04.002, arXiv:1810.08499.

[11] G.J. Feldman, R.D. Cousins, A unified approach to the classical statistical analysis of small signals, Phys. Rev. D 57 (1998) http://dx.doi.org/10.1103/PhysRevD.57.3873, arXiv:physics/9711021.

[12] M. Ackermann, et al., The spectrum of isotropic diffuse gamma-ray emission between 100 MeV and 820 GeV, Astrophys. J. 799 (2015) http://dx.doi.org/10.1088/0004-637X/799/1/86, arXiv:1410.3696.

[13] R. Abbasi, et al., The IceCube high-energy starting event sample: Description and flux characterization with 7.5 years of data, Phys. Rev. D 104 (2021) http://dx.doi.org/10.1103/PhysRevD.104.022002, arXiv:2011.03545.

[14] M.G. Aartsen, et al., Characteristics of the diffuse astrophysical electron and tau neutrino flux with six years of IceCube high energy cascade data, Phys. Rev. Lett. 125 (2020) http://dx.doi.org/10.1103/PhysRevLett.125.121104, arXiv:2001.09520.

[15] K. Fang, J.S. Gallagher, F. Halzen, The TeV diffuse cosmic neutrino spectrum and the nature of astrophysical neutrino sources, Astrophys. J. 933 (2022) http://dx.doi.org/10.3847/1538-4357/ac7649, arXiv:2205.03740.

[16] P. Kornecki, L.J. Pellizza, S. del Palacio, A.L. Müller, J.F. Albacete-Colombo, G.E. Romero, γ-Ray/infrared luminosity correlation of star-forming galaxies, Astron. Astrophys. 641 (2020) http://dx.doi.org/10.1051/0004-6361/202038428, arXiv:2007.07430.

[17] M. Ajello, M. Di Mauro, V. Paliya, S. Garrappa, The γ-ray emission of star-forming galaxies, Astrophys. J. 894 (2020) http://dx.doi.org/10.3847/1538-4357/ab86a6, arXiv:2003.05493.

[18] B. Eichmann, F. Oikonomou, S. Salvatore, R.-J. Dettmar, J. Becker Tjus, Solving the multimessenger puzzle of the AGN-starburst composite galaxy NGC 1068, Astrophys. J. 939 (2022) http://dx.doi.org/10.3847/1538-4357/ac9588, arXiv:2207.00102.

[19] R.R.J. Antonucci, J.S. Miller, Spectropolarimetry and the nature of NGC 1068, Astrophys. J. 297 (1985) http://dx.doi.org/10.1086/163559.

[20] Y. Inoue, D. Khangulyan, A. Doi, On the origin of high-energy neutrinos from NGC 1068: The role of nonthermal coronal activity, Astrophys. J. Lett. 891 (2020) http://dx.doi.org/10.3847/2041-8213/ab7661, arXiv:1909.02239.

[21] A. Kheirandish, K. Murase, S.S. Kimura, High-energy neutrinos from magnetized coronae of active galactic nuclei and prospects for identification of seyfert galaxies and quasars in neutrino telescopes, Astrophys. J. 922 (2021) http://dx.doi.org/10.3847/1538-4357/ac1c77, arXiv:2102.04475.

[22] L.A. Anchordoqui, J.F. Krizmanic, F.W. Stecker, High-energy neutrinos from NGC 1068, PoS ICRC2021, http://dx.doi.org/10.22323/1.395.0993, arXiv:2102.12409.

[23] K. Murase, S.S. Kimura, P. Meszaros, Hidden cores of active galactic nuclei as the origin of medium-energy neutrinos: Critical tests with the MeV Gamma-ray connection, Phys. Rev. Lett. 125 (2020) http://dx.doi.org/10.1103/PhysRevLett.125.011101, arXiv:1904.04226.

[24] J.F. Gallimore, D.J. Axon, C.P. O'Dea, S.A. Baum, A. Pedlar, A survey of kiloparsec-scale radio outflows in radio-quiet active galactic nuclei, Astron. J. http://dx.doi.org/10.1086/504593, arXiv:astro-ph/0604219.

[25] T. Michiyama, Y. Inoue, A. Doi, D. Khangulyan, ALMA detection of parsec-scale blobs at the head of a kiloparsec-scale jet in the nearby seyfert galaxy NGC 1068, Astrophys. J. Lett. 936 (2022) http://dx.doi.org/10.3847/2041-8213/ac8935, arXiv:2208.08533.

[26] M. Mizumoto, T. Izumi, K. Kohno, Kinetic energy transfer from X-Ray ultrafast outflows to millimeter/submillimeter cold molecular outflows in seyfert galaxies, Astrophys. J. 871 (2019) http://dx.doi.org/10.3847/1538-4357/aaf814, arXiv:1812.04316.

[27] V.A. Acciari, et al., Constraints on gamma-ray and neutrino emission from NGC 1068 with the MAGIC telescopes, Astrophys. J. 883 (2019) http://dx.doi.org/10.3847/1538-4357/ab3a51, arXiv:1906.10954.

[28] Y. Merckx, P. Correa, K.D. de Vries, K. Kotera, G.C. Privon, N. van Eijndhoven, Investigating starburst-driven neutrino emission from galaxies in the Great Observatories All-Sky LIRG Survey, Phys. Rev. D 108 (2023) http://dx.doi.org/10.1103/PhysRevD.108.023015, arXiv:2304.01020.

[29] E. Peretti, A. Lamastra, F.G. Saturni, M. Ahlers, P. Blasi, G. Morlino, P. Cristofari, Diffusive shock acceleration at EeV and associated multimessenger flux from ultra-fast outflows driven by active galactic nuclei, Mon. Not. R. Astron. Soc. 526 (2023) http://dx.doi.org/10.1093/mnras/stad2740, arXiv:2301.13689.

[30] K. Fang, E.L. Rodriguez, F. Halzen, J.S. Gallagher, High-energy neutrinos from the Inner Circumnuclear Region of NGC 1068, Astrophys. J. 956 (2023) http://dx.doi.org/10.3847/1538-4357/acee70, arXiv:2307.07121.

[31] A. Marinelli, D. Raudales, A. Ambrosone, M. Chianese, D. Fiorillo, P. Grandi, G. Miele, J. Rodrigo Sacahui, E. Torresi, Neutrino emission from NGC1068: looking at the contribution of the kiloparsec jet, PoS ICRC2023, http://dx.doi.org/10.22323/1.444.1221.

[32] C. Obasi, M. Gómez, D. Minniti, J. Alonso-García, M. Hempel, J.B. Pullen, M.D. Gregg, L.D. Baravalle, M.V. Alonso, B.I. Okere, The globular cluster system of the nearest Seyfert II galaxy Circinus, Astron. Astrophys. http://dx.doi.org/10.1051/0004-6361/202243154, arXiv:2212.05482.

[33] R. Maiolino, A. Krabbe, N. Thatte, R. Genzel, Seyfert activity and nuclear star formation in the circinus galaxy, Astrophys. J. 493 (2) (1998) http://dx.doi.org/10.1086/305150.

[34] M. Stalevski, D. Asmus, K.R.W. Tristram, Dissecting the active galactic nucleus in Circinus – I. Peculiar mid-IR morphology explained by a dusty hollow cone, Mon. Not. R. Astron. Soc. 472 (2017) http://dx.doi.org/10.1093/mnras/stx2227.

[35] K. Murase, C.M. Karwin, S.S. Kimura, M. Ajello, S. Buson, Sub-GeV Gamma rays from nearby seyfert galaxies and implications for coronal neutrino emission, Astrophys. J. Lett. 961 (2) (2024) L34, http://dx.doi.org/10.3847/2041-8213/ad19c5, arXiv:2312.16089.